

Supplemental Data

Experimental Procedures

Brain tumors, primary cultures and gliomaspheres

All primary brain tumors were obtained fresh from the operating room following approved protocols, chopped manually, dissociated with Papain and plated in DMEM-F12 with FBS for adherent culture or seeded at a concentration of 50,000 cell/ml in 1/2-1/3 conditioned medium and DMEM-F12 serum-free medium with 20% BIT 9500 (Stem cell technologies Inc), 10 ng/ml of EGF and 10 ng/ml of FGF-2 for gliomasphere culture. GBM U87 cells (ATCC) were grown as suggested by the supplier. All experiments were done in triplicate. Error bars denoting s.e.m. are shown in all cases except when histograms show ratios. In this case, asterisks denote significant ($p < 0.05$) changes.

Clonal assays and treatments

Gliomaspheres were dissociated and plated at 1 cell/well in 96-well plates containing DMEM-F12, 20% BIT 9500 media with EGF and FGF at a concentration of 10 ng/ml each, with 1/2-1/3 sphere-conditioned media for spheres. Clonal growth was assessed visually with an inverted microscope at 2 weeks (tumor adherent cells) or 10 days (gliomaspheres). ± 400 -600 cloning events in 4-6 96-well plates were performed per experiment and this was repeated in triplicate. N-SHH (100nM; R&D), Cyclopamine (TRC) or Temozolomide (Schering-Plough; kindly provided by P.-Y. Dietrich) were added at the beginning of the culture period for 7 days in media containing 1ng/ml EGF and FGF each. Control cells were treated in the same manner with PBS, tomatidine (Sigma) or DMSO (Fluka). For other uses, cells were treated with SHH, cyclopamine or tomatidine cells in low (2.5%) serum.

siRNAs, transfections and PCR

21nt-long double stranded siRNAs were purified and desalted (Dharmacon Inc). The sequences for the siRNAs were 5'-3': GLI1: AACUCCACAGGCAUACAGGAU; GLI2: AAGAUCUGGACAGGGAUGACU; GLI3: AAUGAGGAUGAAAGUCCUGGA. The second set (Ambion) was: GLI1: GCCCAGAUGAAUCACCAAA; GLI2: CCCUGUCGCCAUUCACAAG; GLI3: GGGCCGUUACCAUUACGAU. Control siRNA with or without an FITC tag: AACGUACGCGGAAUACAACGA. siRNA transfections (0.2 μ M) were performed with Oligofectamine (Invitrogen, Inc). Genes chosen for analyses and quantitative RT-PCR: The genes used to detect the stemness signature in human gliomas were chosen for their association with self-renewal and/or tumorigenicity. These were the following with indicative references: *CD133* (refs. 1-3); *OLIG2* (refs. 4,5); *BMI1* (refs. 6-10); *BREVICAN* (11,12; *BCAN*); *NANOG* and *OCT4* (refs. 13-17); *SOX2* (refs. 17-20); *PTEN* (21-26); *ABCG2* (refs. 27-29); *PDGFRA* (30-33); *NEUROD1* (*NRD1*;ref. 34); *NESTIN* (35-37); *NOTCH1* (refs. 38-41); *MELK* (42). qPCR primers were 5'->3': GLI2-F: CACCGCTGCTCAAAGAGAA, GLI2-R: TCTCCACGCCACTGTCATT; GLI3-F: CGAACAGATGTGAGCGAGAA, GLI3-R: TTGATCAATGAGGCCCTCTC; PTCH1-F: CCACAGAAGCGCTCCTACA, PTCH1-R: CTGTAATTTGCCCCCTTCC; SHH-2F: TCCAAGGCACATATCCACTG, SHH-2R: CCAGGAAAGTGAGGAAGTCG; HIP-F: CCCACACTTCAACAGCACCA, HIP-R: GCTTTGTCACAGGACTTTGC; CD133-F: GCCACCGCTCTAGATACTGC, CD133-R: TGTGTGATGGGCTTGTCAT; NOTCH1-F: GGCCACCTGGGCCGGAGCTTC, NOTCH1-R: GCGATCTGGGACTGCATGCTG. SOX-2-F: ACACCAATCCCATCCACACT, SOX-2-R: GCAAACCTCCTGCAAAGCTC; MELK-F: CAGGCAAACAATGGAGGATT, MELK-R: TGTCTGTGAATGGGGTAGCA; CD44-F: AAGGTGGAGCAAACACAACC, CD44-R: AGCTTTTTCTTCTGCCACA; BMI1SQ-F: GCAGCAATGACTGTGATG, BMI1SQ-R: AGTCCATCTCTCTGGTGAC; ABCG2-F: CACCTTATTGGCCTCAGGAA, ABCG2-R:

CCTGCTTGGAAGGCTCTATG; NANOG-F: GTCCCGGTCAAGAAACAGAA, NANOG-R:
 TGCATCACACCATTGCTATT; OCT4-F: ATTCAGCCAAACGACCATCT, OCT4-R:
 TTGCCTCTCCACTCGGTTCTC; EGFR-F: CAGCGCTACCTTGTCATTCA, EGFR-R:
 AGCTTTGCAGCCCATTTCTA; PTEN-F: ACCAGGACCAGAGGAAACCT, PTEN-R:
 GCTAGCCTCTGGATTTGACG; PCNA-F: GGCTCTAGCCTGACAAATGC, PCNA-R:
 GCCTCCAACACCTTCTTGAG; YKL40-F: TCAAGAACAGGAACCCCAAC, YKL40-R:
 AAATTCGGCCTTCATTTCTC; BCAN-F: GGAATCAACGACAGGACCAT, BCAN-R:
 GCAGGTGTAGGACAGGTGGT; NCAM-F: GTGGACTCGACCAGAGAAGC, NCAM-R:
 CTTTGGGGCATATTGCACTT; GFAP-F: ACATCGAGATCGCCACCTAC, GFAP-R:
 ATCTCCACGGTCTTCACCAC; DCX-F: GACAGCCCACTCTTTTGAGC, DCX-R:
 TGGGTTTCCCTTCATGACTC; NEUD1-F: GCCCCAGGGTTATGAGACTA, NEUD1-R:
 GCTCCTCGTCCTGAGAACTG; OLIG2-F: CAGAAGCGCTGATGGTCATA, OLIG2-R:
 TCGGCAGTTTTGGGTTATTC; VIM-F: CCCTCACCTGTGAAGTGGAT, VIM-R:
 TCCAGCAGCTTCCTGTAGGT; at 60°C and NESTIN-s:
 GGCAGCGTTGGAACAGAGGTTGGA, NESTIN-a: CTCTAAACTGGAGTGGTCAGGGCT;
 NUCLEOSTEMIN-s : CAAAGCCAAGTCGGGCAAAC, NUCLEOSTEMIN-a:
 CCTGAGGACATCTGCAACCAA at 56°C, Primers for *GAPDH* and *GLII* were as described
 respectively (30,43,44). Quantitative RT-PCR was performed using the iQ[™] SYBR Green
 supermix (Biorad) according to manufacturers' instructions at 60°C.

Immunohistochemistry in situ hybridization

Immunocytochemistry used mouse anti-BrdU (R&D Systems), rabbit anti-Capase-3 (Cell
 signaling), rabbit anti-GFAP (Sigma), mouse anti-Nestin (R&D Systems) and rabbit anti-GFP
 primary antibodies (Molecular Probes) with FITC- or rhodamine-conjugated secondary antibodies
 (Molecular Probes). Stained cells were observed by Zeiss Axiocam optical and LSM MEta 510

confocal microscopy. In situ hybridizations with digoxigenin-labeled antisense RNA probes for *GLI1*, *PTCH1* and *SHH* were as described (30).

Proliferation assays

U87 cells were given a 2 h pulse of BrdU (Sigma) at 4 μ g/ml, while primary tumor and gliomaspheres were given 16 h pulse. The length of the gliomasphere cell cycle length was estimated to be \pm 36h. Visualization of new DNA synthesis was revealed by anti-BrdU indirect immunofluorescence on adherent cultures directly with an Axiophot and in whole gliomaspheres with Confocal Z-stacks of an LSM510 Meta after placing them for 30-60' before fixation on adherent coated dishes. Cell viability was tested by the colorimetric MTT assay (Promega) in 96-well plates or by trypan blue exclusion after dissociation.

CD133 FACS staining sorting

Gliomasphere cultures were dissociated and labeled with CD133 antibody as previously described (1,3). Briefly, spheres were dissociated and labeled with CD133/2 (293C3)-PE antibody (Miltenyi Biotech) and the expression level was analysed on a Beckton Dickinson FACSCalibur (BD Bioscience) for measuring abundance. For sorting, dissociated sphere were labeled with CD133/1-microbeads (MiltenyiBiotech) at a concentration of 1 μ l/10⁶ cells according to manufacturers' instructions. Magnetic bead-antibody-antigen separation was performed using the possel-s program on an autoMACS machine.

Mouse xenografts of human gliomas

Cells infected with appropriate lentiviral vectors (GFP- or beta gal-expressing) to allow tracing in vivo. \pm 72 after infection (to allow for expression of the integrated lentiviral vectors) cells were dissociated and adjusted at the desired concentration in 2 μ l in cold HBSS. For subcutaneous

xenografts, U87 cells were injected (2×10^6 cells) on each back side of each mouse. As soon as the tumor was palpable, cyclodextrin-conjugated cyclopamine or cyclodextrin carrier alone (Sigma) at 10mg/kg were injected in the immediate vicinity or intratumorally when possible twice daily. For intracranial grafts, gliomaspheres (10^4 or 10^5 cells) were implanted at coordinates X= -2, Y=0, Z=-2 relative to the bregma point with a stereotaxic apparatus. 2 weeks after injection, systemic intraperitoneal injection of cyclodextrin-conjugated cyclopamine or cyclodextrin carrier alone at 10mg/kg were done twice daily.

Lentiviral transduction and construction

pLVCTH lentiviral vectors containing an H1 promoter to drive shRNA expression were grown as described (45). The shRNA sequence targeting SMOH was: AGTGTTGACTGTGTCATTA. The VSV-G pseudotyped lentiviral vectors LV-control (pLV-CTH parental vector) and the derived LV-shSMOH were produced by transient cotransfection of three plasmids into 293T cells using approved protocols. Conditional expression of the shRNA from LV-shSMOH was accomplished after coinfection with LV-rtTA-KRAB (45). This lentiviral vector expresses a recombinant tet-repressor-KRAB protein that silences the promoters in LV-shSMOH. Only upon doxycyclin (DOX) addition ($5 \mu\text{g/ml}$ in the culture media renewed daily for in vitro use, or 2g/l in the drinking water with 5% sucrose plus $20 \mu\text{g/ml}$ IP daily for in vivo use) does the trTR-KRAB protein is rendered nonfunctional and transcription of the shRNA begins.

Supplementary References

- 1 Uchida, N., Buck, D.W., He, D., Reitsma, M.J., Masek, M., Phan, T.V., Tsukamoto, A.S., Gage, F.H., Weissman, I.L. (2000). Direct isolation of human central nervous system stem cells. *Proc Natl Acad Sci U S A*. 97, 14720-14725.
- 2 Singh, S.K. Clarke, I.D., Terasaki, M., Bonn, V.E., Hawkins, C., Squire, J., Dirks, P.B. (2003). Identification of a cancer stem cell in human brain tumors. *Cancer Res*. 63, 5821-5828.

- 3 Singh, S.K., Hawkins, C., Clarke, I.D., Squire, J.A., Bayani, J., Hide, T., Henkelman, R.M., Cusimano, M.D., Dirks, P.B. (2004). Identification of human brain tumour initiating cells. *Nature* 432, 396-401.
- 4 Lu, Q.R., Park, J.K., Noll, E., Chan, J.A., Alberta, J., Yuk, D., Alzamora, M.G., Louis, D.N., Stiles, C.D., Rowitch, D.H., Black, P.M. (2001). Oligodendrocyte lineage genes (OLIG) as molecular markers for human glial brain tumors. *Proc Natl Acad Sci U S A* 98, 10851-10856.
- 5 Bouvier, C., Bartoli, C., Aguirre-Cruz, L., Virard, I., Colin, C., Fernandez, C., Gouvernet, J., Figarella-Branger, D. (2003). Shared oligodendrocyte lineage gene expression in gliomas and oligodendrocyte progenitor cells. *J Neurosurg* 99, 344-350.
- 6 Leung, C., Lingbeek, M., Shakhova, O., Liu, J., Tanger, E., Saremaslani, P., Van Lohuizen, M., Marino, S. (2004). *Bmi1* is essential for cerebellar development and is overexpressed in human medulloblastomas. *Nature* 428, 337-341.
- 7 Molofsky, A.V., He, S., Bydon, M., Morrison, S.J., Pardal, R. (2005). *Bmi-1* promotes neural stem cell self-renewal and neural development but not mouse growth and survival by repressing the p16Ink4a and p19Arf senescence pathways. *Genes Dev* 19, 1432-1437.
- 8 Bruggeman, S.W., Valk-Lingbeek M.E., van der Stoop, P.P., Jacobs J.J, Kieboom, K., Tanger, E., Hulsman, D., Leung, C., Arsenijevic, Y., Marino, S., van Lohuizen, M. (2005). *Ink4a* and *Arf* differentially affect cell proliferation and neural stem cell self-renewal in *Bmi1*-deficient mice. *Genes Dev* 19, 1438-1443.
- 9 Zencak, D., Lingbeek, M., Kostic, C., Tekaya, M., Tanger, E., Hornfeld, D., Jaquet, M., Munier, F.L., Schorderet, D.F., van Lohuizen, M., Arsenijevic, Y. (2005). *Bmi1* loss produces an increase in astroglial cells and a decrease in neural stem cell population and proliferation. *J Neurosci* 25, 5774-5783.
- 10 Lee, T.I., Jenner, R.G., Boyer, L.A., Guenther, M.G., Levine, S.S., Kumar, R.M., Chevalier, B., Johnstone, S.E., Cole, M.F., Isono, K., Koseki, H., Fuchikami, T., Abe, K., Murray, H.L., Zucker, J.P., Yuan, B., Bell, G.W., Herbolsheimer, E., Hannett, N.M., Sun, K., Odom, D.T., Otte, A.P., Volkert, T.L., Bartel, D.P., Melton, D.A., Gifford, D.K., Jaenisch, R., Young, R.A. (2006). Control of developmental regulators by Polycomb in human embryonic stem cells. *Cell* 125, 301-313.
- 11 Viapiano, M.S., Bi W.L., Piepmeier, J., Hockfield, S., Matthews, R.T. (2005). Novel tumor-specific isoforms of *BEHAB/brevican* identified in human malignant gliomas. *Cancer Res* 65, 6726-6733.
- 12 Phillips, H.S., Kharbanda, S., Chen, R., Forrest, W.F., Soriano, R.H., Wu, T.D., Misra, A., Nigro, J.M., Colman, H., Soroceanu, L., Williams, P.M., Modrusan, Z., Feuerstein, B.G., Aldape, K. (2006). Molecular subclasses of high-grade glioma predict prognosis, delineate a pattern of disease progression, and resemble stages in neurogenesis. *Cancer Cell* 9, 157-173.
- 13 Boiani, M. and Scholer, H.R. (2005). Regulatory networks in embryo-derived pluripotent stem cells. *Nat. Rev. Mol. Cel. Biol.* 6, 872-884.

- 14 Boyer, L.A., Lee T.I., Cole, M.F., Levine, S.S, Zucker, J.P., Guenther, M.G., Kumar, R.M., Murray, H.L., Jenner, R.G., Gifford, D.K., Melton, D.A., Jaenisch, R., Young, R.A. (2005). Core transcriptional regulatory circuitry in human embryonic stem cells. *Cell* *122*, 947-956.
- 15 Loh, Y.H., Wu, Q., Chew, J.L., Vega, V.B., Zhang, W., Chen, X., Bourque, G., George, J., Leong, B., Liu, J., Wong, K.Y., Sung, K.W., Lee, C.W., Zhao, X.D., Chiu, K.P., Lipovich, L., Kuznetsov, V.A., Robson, P., Stanton, L.W., Wei, C.L., Ruan, Y., Lim, B., Ng, H.H. (2006). The Oct4 and Nanog transcription network regulates pluripotency in mouse embryonic stem cells. *Nat Genet* *38*, 431-440.
- 16 Silva, J., Chambers, I., Pollard, S., Smith, A. (2006). Nanog promotes transfer of pluripotency after cell fusion. *Nature* *441*, 997-1001.
- 17 Ivanova, N., Dobrin, R., Lu, R., Kotenko, I., Levorse, J., DeCoste, C., Schafer, X., Lun, Y., Lemischka, I.R. (2006). Dissecting self-renewal in stem cells with RNA interference. *Nature* *442*, 533-538.
- 18 Avilion, A.A., Nicolis, S.K., Pevny, L.H., Perez, L., Vivian, N., Lovell-Badge, R. (2003). Multipotent cell lineages in early mouse development depend on SOX2 function. *Genes Dev* *17*, 126-140.
- 19 Ellis, P., Fagan, B.M., Magness, S.T., Hutton, S., Taranova, O., Hayashi, S., McMahon, A., Rao, M., Pevny, L. (2004). SOX2, a persistent marker for multipotential neural stem cells derived from embryonic stem cells, the embryo or the adult. *Dev Neurosci* *26*, 148-165.
- 20 Taranova, O.V., Magness, S.T., Fagan, B.M., Wu, Y., Surzenko, N., Hutton, S.R., Pevny, L.H. (2006). SOX2 is a dose-dependent regulator of retinal neural progenitor competence. *Genes Dev* *20*, 1187-1202.
- 21 He, X.C., Zhang, J., Tong, W.G., Tawfik, O., Ross, J., Scoville, D.H., Tian, Q., Zeng, X., He, X., Wiedemann, L.M., Mishina, Y., Li, L. (2004). BMP signaling inhibits intestinal stem cell self-renewal through suppression of Wnt-beta-catenin signaling. *Nat Genet* *36*, 1117-1121.
- 22 Zhang, J., Grindley, J.C., Yin, T., Jayasinghe, S., He, X.C., Ross, J.T., Haug, J.S., Rupp, D., Porter-Westpfahl, K.S., Wiedemann, L.M., Wu, H., Li, L. (2006). PTEN maintains haematopoietic stem cells and acts in lineage choice and leukaemia prevention. *Nature* *441*, 518-522.
- 23 Yilmaz, O.H., Valdez, R., Theisen, B.K., Guo, W., Ferguson, D.O., Wu, H., Morrison, S.J. (2006). Pten dependence distinguishes haematopoietic stem cells from leukaemia-initiating cells. *Nature* *441*, 475-482.
- 24 Wang, S., Garvia, A.J., Wu, M., Lawson, D.A., Witte, O.N., Wu, H. (2006) Pten deletion leads to the expansion of a prostatic stem/progenitor cell subpopulation and tumor initiation. *Proc Natl Acad Sci U S A* *103*, 1480-1485.

- 25 Groszer, M., Erickson, R., Scripture-Adams, D.D., Lesche, R., Trumpp, A., Zack, J.A., Kornblum, H.I., Liu, X., Wu, H. (2001). Negative regulation of neural stem/progenitor cell proliferation by the Pten tumor suppressor gene in vivo. *Science* *94*, 2186-2189.
- 26 Groszer, M., Erickson, R., Scripture-Adams, D.D., Dougherty, J.D., Le Belle, J., Zack, J.A., Geschwind, D.H., Liu, X., Kornblum, H.I., Wu, H. (2006). PTEN negatively regulates neural stem cell self-renewal by modulating G0-G1 cell cycle entry. *Proc Natl Acad Sci U S A* *103*, 111-116.
- 27 Islam, M.O., Kanemura, Y., Tajria, J., Mori, H., Kobayashi, S., Hara, M., Yamasaki, M., Okano, H., Miyake, J. (2005). Functional expression of ABCG2 transporter in human neural stem/progenitor cells. *Neurosci. Res.* *52*, 75-82.
- 28 Patrawala, L., Calhoun, T., Schneider-Broussard, R., Zhou, J., Claypool, K., Tang, D.G. (2005). Side population is enriched in tumorigenic, stem-like cancer cells, whereas ABCG2+ and ABCG2- cancer cells are similarly tumorigenic. *Cancer Res.* *65*, 6207-6219.
- 29 Zhou, S., Schuetz, J.D., Bunting, K.D., Colapietro, A.M., Sampath, J., Morris, J.J., Lagutina, I., Grosveld, G.C., Osawa, M., Nakauchi, H., Sorrentino, B.P. (2001). The ABC transporter Bcrp1/ABCG2 is expressed in a wide variety of stem cells and is a molecular determinant of the side-population phenotype. *Nat Med.* *7*, 1028-1034.
- 30 Dahmane, N., Sanchez, P., Gitton, Y., Palma, V., Sun, T., Beyna, M., Weiner, H., Ruiz I Altaba, A. (2001). The SHH-GLI pathway regulates dorsal brain growth and tumorigenesis. *Development* *128*, 5201-5212.
- 31 Dai, C., Celestino, J.C., Okada, Y., Louis, D.N., Fuller, G.N., Holland, E.C. (2001) PDGF autocrine stimulation dedifferentiates cultured astrocytes and induces oligodendrogliomas and oligoastrocytomas from neural progenitors and astrocytes in vivo. *Genes Dev.* *15*, 1913-1925.
- 32 MacDonald, T.J., Brown, K.M., LaFleur, B., Peterson, K., Lawlor, C., Chen, Y., Packer R.J., Cogen, P., Stephan, D.A. (2001). Expression profiling of medulloblastoma: PDGFRA and the RAS/MAPK pathway as therapeutic targets for metastatic disease. *Nat Genet* *29*, 143-152.
- 33 Jackson, E.L., Garcia-Verdugo, J.M., Gil-Perotin, S., Roy, M., Quinones-Hinojosa, A., Vandenberg, S., Alvarez-Buylla, A. (2006). PDGFR α -Positive B cells are neural Stem Cells in the Adult SVZ that form glioma-like growths in response to increased PDGF signaling. *Neuron* *51*, 187-199.
- 34 Rostomily, R.C., Bermingham-McDonogh, O., Berger, M.S., Tapscott, S.J., Reh, T.A., Olson, J.M. (1997). Expression of neurogenic basic helix-loop-helix genes in primitive neuroectodermal tumors. *Cancer Res.* *57*, 3526-3531.
- 35 Lendahl, U., Zimmerman, L.B., McKay, R.D. (1990). CNS stem cells express a new class of intermediate filament protein. *Cell* *60*, 585-595.

- 36 Rao, G., Pedone, C.A., Valle, L.D., Reiss, K., Holland, E.C., Fults, D.W. (2004). Sonic hedgehog and insulin-like growth factor signaling synergize to induce medulloblastoma formation from nestin-expressing neural progenitors in mice. *Oncogene* 23, 6156-6162.
- 37 Assanah, M., Lochhead, R., Ogden, A., Bruce, J., Goldman, J., Canoll, P. (2006). Glial progenitors in adult white matter are driven to form malignant gliomas by platelet-derived growth factor-expressing retroviruses. *J Neurosci* 26, 6781-6790.
- 38 Purow, B.W., Haque, R.M., Noel, M.W, Su, Q., Burdick, M.J., Lee, J., Sundaresan, T., Pastorino, S., Park, J.K., Mikolaenko, I., Maric, D., Eberhart, C.G., Fine, H.A. (2005) Expression of Notch-1 and its ligands, Delta-like-1 and Jagged-1, is critical for glioma cell survival and proliferation. *Cancer Res.* 65, 2353-2363.
- 39 Guentchev, M., McKay, R.D. (2006). Notch controls proliferation and differentiation of stem cells in a dose-dependent manner. *Eur J Neurosci* 23, 2289-2296.
- 40 Hallahan, A.R., Pritchard, J.I., Hansen, S., Benson, M., Stoeck, J., Hatton, B.A., Russell, T.L., Ellenbogen, R.G., Bernstein, I.D., Beachy, P.A., Olson, J.M. (2004). The SmoA1 mouse model reveals that notch signaling is critical for the growth and survival of sonic hedgehog-induced medulloblastomas. *Cancer Res.* 64, 7794-7800.
- 41 Hitoshi, S., Alexson, T., Tropepe, V., Donoviel, D., Elia, A.J., Nye, J.S., Conlon, R.A., Mak, T.W., Bernstein, A., van der Kooy, D. (2002). Notch pathway molecules are essential for the maintenance, but not the generation, of mammalian neural stem cells. *Genes Dev* 16, 846-858.
- 42 Nakano, I., Paucar, A.A., Bajpai, R., Dougherty, J.D., Zewail, A., Kelly, T.K., Kim, K.J., Ou, J., Groszer, M., Imura, T., Freije, W.A., Nelson, S.F., Sofroniew, M.V., Wu, H., Liu, X., Terskikh, A.V., Geschwind, D.H., Kornblum, H.I. (2005). Maternal embryonic leucine zipper kinase (MELK) regulates multipotent neural progenitor proliferation. *J. Cell Biol.* 170, 413-427.
- 43 Palma, V. and Ruiz i Altaba, A. (2004). Hedgehog-GLI signaling regulates the behavior of cells with stem cell properties in the developing neocortex. *Development* 131, 337-345.
- 44 Sanchez, P., Hernandez, A.M., Stecca, B., Kahler, A.J., DeGueme, A.M., Barrett, A., Beyna, M., Datta, M.W., Datta, S., Ruiz i Altaba, A. et al. (2004). Inhibition of prostate cancer proliferation by interference with Hedgehog-GLI1 signaling. *Proc Nat Acad Sci USA* 101,12561-12566.
- 45 Wiznerowicz, M., Trono, D. (2003). Conditional suppression of cellular genes: lentivirus vector-mediated drug-inducible RNA interference. *J. Virol* 77, 8957-8961.

Supplemental Figures

Supplemental Figure 1. Summary of brain tumors used in this study and their

expression of SHH-GLI pathway components. A) Grade, age, gender and location of primary brain tumors, normal epileptic samples and the U87 cell line used.

B-D) Summary of the expression levels of *GLI1* and *PTCH1* (B), *GLI2* and *GLI3* (C) and *SHH* and *HIP1* (D) in different brain tumors as determined by qPCR. Note the ubiquitous activity of the HH-GLI pathway as denoted by the increased levels of *GLI1* in all tumor types and two HH-GLI regulated genes: *PTCH1* and *HIP1*. The expression levels are the relative ratio of gene expression over that of *GAPDH*.

Supplemental Figure 2. Quantitative changes in gene expression in fresh tumors

determined by qPCR. This data was used to generate Fig. 1A. All numbers denote relative fold expression over *GAPDH*, used as ubiquitous control. The bottom box includes the values of three normal cortical samples from a hemispherectomy of an epileptic patient used to determine the up and down thresholds for normal expression. The thresholds themselves were then arbitrarily set close to the up and down limit values observed for the control brain samples but always slightly expanding the normal range. This then allowed us to consider as within the normal range any value in tumor samples that was very close to the three normal values in order to avoid over-representing in the overexpressed set any value that was very close to the normal range.

Supplemental Figure 3. Poor correlation of a set of recently defined glioma markers with glioma grade or type. The three glioma classes reported (12) are mesenchymal,

characterized by high *YKL40* and *CD44* expression, Proneural, characterized by high *BCAN* and low *MELK* expression and Proliferative, characterized by high *CD133*, *PCNA* and low *GFAP* expression (12). Thresholds were obtained as in Supplementary Fig. 2 from normal cortical samples. All numbers denote relative fold expression over *GAPDH*, used as ubiquitous control. Only 6/27 tumors matched: Mesenchymal: GBM5,6,7; Proneural: no match; Proliferative: GBM9.

Supplemental Figure 4. Inhibitory effects of cyclopamine treatment on glioma stem cell cultures and U87 glioma cells.

A) Growth inhibition of three glioma stem cell cultures treated over 9 days and measured by the viability MTT assay. Histograms show cyc/tom ratios each at 10 μ M and asterisks denote significant ($p < 0.05$) changes. B) Inhibition of *GLI1* transcription in U87 cells 4h after treatment with 10 μ M cyclopamine. C) Death of U87 cells induced by treatment with cyclopamine (10 μ M) and recovery of the culture following removal of the drug after 4 days for its ethanol solvent.

Supplemental Figure 5. Effects of an independent set of siRNAs targeting different regions in *GLI1*, *GLI2* and *GLI3* mRNAs and effects on U87 survival.

A) Inhibition of cell proliferation shown as a percentage ratio of reduction of BrdU+ cells in each individual GLI siRNA over a control, unrelated siRNA (siC). Asterisks denote significant ($p < 0.05$) changes. B) Reduction of *GLI1*, *GLI2* or *GLI3* mRNA levels in U87 cells and GBM-8 adherent cells after lipofection with the appropriate siRNAs and measured by qPCR, over *GAPDH* values, shown as ratios over a control siRNA. Gliomaspheres cannot be lipofected to usable levels. C) Long-term treatment of U87 glioma cells with siRNA *GLI1* (siGLI1), but not siRNA *GLI2* (siGLI2) or siRNA control (siC), leads to cell death as measured by retention of trypan blue. Cells were lipofected

anew every other day to maintain high levels of siRNAs in them. Asterisks denote significant ($p < 0.05$) changes.

Supplemental Figure 6. Effects of temozolomide on glioma stem cell cultures.

A-D) Concentration-dependent inhibition of cell proliferation (A,C) and increase in apoptotic death (B,D), measured by BrdU incorporation (A,C) and activated Caspase-3 immunostaining (B,D), by temozolomide (TMZ) treatment in U87 cells (A,B) and three glioma stem cell cultures (C,D). E) Additive and synergistic effects on the induction of apoptotic cell death after treatment with intermediate doses of TMZ and cyclopamine on three glioma stem cell cultures and U87. Histograms show ratios of TMZ versus DMSO treated samples (A-D) or over tomatidine treated samples for cycloapmine (E). Asterisks denote significant ($p < 0.05$) changes as compared to cyclopamine alone. F,G) Long-term treatment and recovery of gliomasphere cultures after treatment with cyclopamine (F) or TMZ (G) for different number of days (d) as measured by trypan blue exclusion in live cells. Note that only after cyclopamine treatment there is significant ($p < 0.05$) non-recovery of the cultures (asterisks).

Supplemental Figure 7. In situ hybridization of intracerebral human gliomas in nude mice.

Dissociated GBM-8 gliomaspheres were injected into the brains of nude mice. The brains harboring the infiltrative gliomas were collected after ± 2 -months, sectioned with a cryostat and frozen sections hybridized with human antisense RNA probes to localize the expression of *GLII*, *SHH* and *PTCH1*. The human probes do not pick up the mouse mRNAs. Specific hybridization was revealed with NBT/BCIP yielding a blue precipitate (top row). As control, sense probes gave no signal (not shown) and the control, uninjected side of the mouse brain implanted with gliomaspheres contralaterally also did not show expression (bottom row). H&E staining was used (left column) to show cellularity, which increased in the tumor (top).

Scale bar = 70µm for all panels.

Supplemental Figure 8. Gene expression in glioma stem cell cultures determined by qPCR.

The data shown here were used to generate Fig. 3A. Calculation of the mean included all samples except outliers when marked by an asterisk. Gene expression values are shown relative to that of *GAPDH*.

Supplemental Figure 9. Effects of SHH on glioma stem cell self-renewal. N-SHH (at 100nM; R&D Systems) or PBS used as control were used to treat whole glioma stem cell cultures (A) or CD133+ cells glioma stem cells (B) for 7 days. The gliomaspheres were then washed and tested for the formation of secondary spheres without SHH after dissociation. Histograms show ratios of SHH- versus PBS-treated samples and asterisks denote significant ($p < 0.05$) changes. CD133+ cells were FACS-sorted from existing stem cell cultures (cultured) or from a fresh GBM from the operating room (fresh).

Supplemental Figure 10. Gene expression in CD133+ FACS-sorted glioma stem cells.

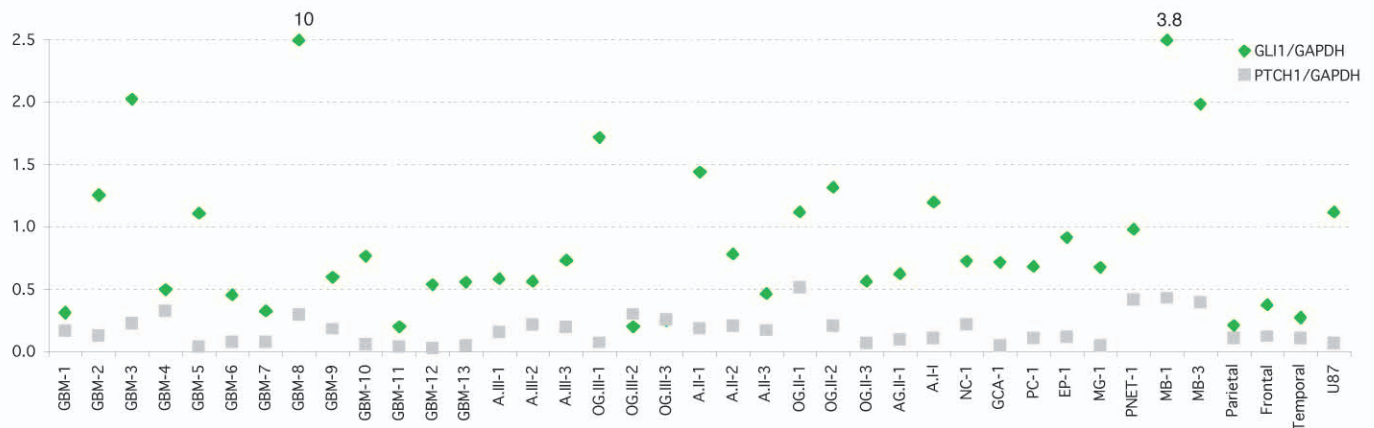
Expression profile of selected genes in CD133+ gliomasphere cells as compared with the CD133⁻ population. The qPCR data shown in (A) were used to generate (B). The numbers in (A) represent the ratio of gene expression values in CD133+ over CD133⁻ cells. In each case, gene expression was expressed as the relative value over that of *GAPDH*. B) White denotes values within 30% of equal expression in CD133+ vs CD133⁻ cells, red for 40% enrichment or more and light blue for 40% impoverishment or more in CD133+ cells. *SHH* and *NOTCH1* as well as stemness genes are highlighted and values boxed. Values for clonogenicity and number of CD133+ cells is also given for the different stem cell cultures (B, bottom).

A

Table of brain tumors and normal tissues used in this study

GBM-1	Glioblastomamultiforme	52 M	righttemporal
GBM-2	"	n/a	n/a
GBM-3	"	50 M	frontal
GBM-4	"	51 F	parieto-occipital(ventriculartrigone)
GBM-5	"	56 M	occipitaleft
GBM-6	"	64 F	frontaleft
GBM-7	"	51 M	occipitaireft
GBM-8	"	51 F	parietaireft
GBM-9	"	70 M	temporaleft
GBM-10	"	66 F	n/a
GBM-11	"	74 M	temporaleft
GBM-12	"	50 M	temporaleft
GBM-13	"	46 M	n/a
A.III-1	AstrocytomagradeIII	33 M	leftfrontal
A.III-2	"	30 M	n/a
A.III-3	"	34 F	temporaleft
OG.III-1	OligodendrogliomagradeIII	54 M	frontaleft(recurrence)
OG.III-2	"	68 M	temporaleft(recurrence)
OG.III-3	"	83 M	n/a
A.II-1	AstrocytomagradeII	24 M	temporaleftlobe
A.II-2	"	31 F	n/a
A.II-3	"	47 M	n/a
OG.II-1	OligodendrogliomagradeII	41 F	frontaleft
OG.II-2	"	n/a	n/a
OG.II-3	"	55 M	frontaireft
AG.II-1	GenistocyticaastrocytomagradeII	56 M	fronto-tempo-insula(peri-sylvian)
A.I-I	Juvenilepylocyticaastrocytoma(gradeI)	n/a	n/a
NC-1	neurocytoma	2 M	3rdventricle
GCA-1	giantcellastrocytoma	12 M	sub-ependymallateralventricle
PC-1	pineacytoma	n/a	n/a
EP-1	ependymoma	6 M	cerebellum
EP-2	"	6 M	cerebellum
MG-1	meningioma	70 M	n/a
PNET-1	PNET	10 n/a	frontallobe
MB-1	medulloblastoma	17 M	cerebellum
MB-2	"	3 F	cerebellum
MB-3	"	n/a	n/a
Parietalex	epilepticnormalbrain	5 M	parietal
Frontal	"	5 M	frontal
Temporal	"	5 M	temporal
U87	gliomacellline		

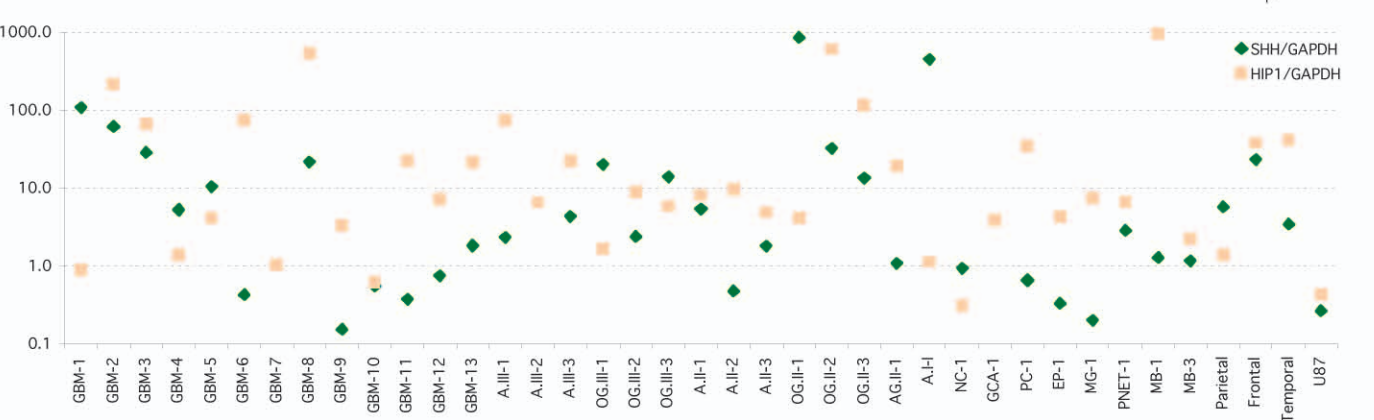
B



C



D



	GLI1	GLI2	GLI3	PTCH1	SHH	NESTIN	NOTCH1	CD133	OLIG2	BMI1	BCAN	OCT4	NANOG	PTEN	ABC2	PDGFRA	SOX2	NRD1	MELK	EGFR	GFAP	PCNA
GBM-12	0.54	0.49	1.77	0.03	0.75	1.17	0.96	ND	0.20	ND	ND	0.04	0.15	0.005	ND	ND	0.23	0.007	0.01	ND	ND	0.03
GBM-1	0.32	0.68	1.58	0.17	109.3	3.58	0.36	0.87	0.32	0.40	0.10	0.22	0.50	1.00	0.24	0.01	3.01	0.05	0.02	0.15	8.86	0.23
GBM-11	0.20	0.16	0.60	0.05	0.38	3.07	0.11	5.02	0.62	0.25	0.04	0.13	0.21	0.25	0.05	0.10	5.22	0.14	0.02	0.08	39.35	0.10
GBM-10	0.77	0.34	1.58	0.06	0.56	1.71	0.20	8.11	0.37	0.18	0.06	0.15	0.44	0.32	0.07	0.12	5.64	0.02	0.02	0.21	117.2	0.11
GBM-9	0.60	0.17	0.38	0.19	0.16	2.38	0.31	4.37	0.32	0.99	0.03	0.33	0.76	1.20	0.20	0.07	2.55	4.76	0.01	0.02	17.95	0.40
GBM-2	1.26	1.95	2.17	0.13	61.9	3.13	0.36	5.98	1.13	0.49	0.10	0.17	0.52	0.60	0.17	0.01	1.74	0.29	0.02	0.27	235.0	0.20
GBM-8	9.97	15.42	3.36	0.30	21.71	1.82	0.70	0.16	0.13	0.11	0.13	0.20	0.25	0.47	0.02	1.74	138.7	0.06	0.04	0.14	54.0	0.22
GBM-13	0.56	0.17	1.14	0.06	1.84	27.06	0.15	8.83	0.70	0.26	0.05	0.33	1.45	0.47	0.14	0.04	1.40	0.10	0.02	0.07	58.4	0.12
GBM-7	0.33	0.47	1.34	0.08	ND	19.60	1.06	43.55	0.88	0.61	0.20	0.25	0.49	0.87	0.19	0.15	4.15	0.09	0.08	0.28	254.8	0.35
GBM-3	2.02	2.79	1.42	0.23	28.3	11.10	0.10	3.67	7.38	0.60	0.15	0.23	0.47	0.78	0.28	0.13	5.16	0.96	0.05	0.34	206.1	0.32
OG.III-1	1.72	ND	1.11	0.08	20.1	7.84	7.23	ND	1.42	0.63	0.10	1.04	3.13	0.63	ND	0.27	2.79	0.83	0.10	0.02	74.3	0.51
GBM-5	1.11	0.53	1.39	0.04	10.56	2.41	0.62	4.70	1.26	0.41	0.18	0.36	0.65	1.12	0.41	0.45	5.33	0.25	0.03	0.12	220.0	0.53
GBM-4	0.50	0.89	1.02	0.33	5.30	2.43	1.21	1.47	1.17	0.42	0.35	0.44	1.02	1.25	0.53	0.46	6.72	0.22	0.09	0.19	179.0	0.38
GBM-6	0.46	1.52	1.67	0.08	0.43	13.93	0.51	11.42	1.74	1.02	0.25	0.73	1.44	1.61	0.83	0.86	50.72	1.12	0.07	0.28	553.5	0.74
A.III-3	0.73	0.68	1.35	0.20	4.35	6.62	0.88	2.66	2.69	0.69	0.29	0.48	1.37	1.75	0.53	1.05	4.85	0.74	0.03	0.24	134.5	0.41
A.III-1	0.59	0.46	1.62	0.16	2.34	8.44	2.00	9.50	10.38	2.09	0.63	0.96	2.27	2.19	0.70	1.64	8.06	1.74	0.35	0.32	651.6	0.79
A.III-2	0.56	1.67	3.46	0.22	ND	37.13	0.41	15.68	11.23	2.03	0.42	1.17	2.56	2.80	0.92	1.70	115.5	1.19	0.12	0.47	482.9	1.13
OG.III-2	0.20	2.81	1.74	0.30	2.42	4.23	1.00	20.22	18.02	2.04	0.50	0.74	1.52	3.47	1.53	1.75	13.40	1.62	0.07	0.30	444.4	0.74
OG.III-3	0.25	1.28	1.72	0.26	14.1	43.96	0.26	9.97	13.06	1.59	0.44	0.56	1.82	2.45	0.96	1.82	132.6	1.36	0.05	0.30	88.7	0.70
OG.II-3	0.57	0.81	1.05	0.07	13.6	6.78	1.84	12.45	10.80	1.73	0.86	1.52	2.64	3.37	1.20	6.31	20.04	2.58	0.04	0.66	561.6	1.00
AG.II-1	0.63	3.14	2.87	0.10	1.10	21.27	0.78	108.3	1.85	1.97	0.16	0.63	0.27	2.29	0.75	0.28	13.02	0.21	0.03	0.63	549.5	1.04
A.II-1	1.44	0.26	1.11	0.19	5.48	8.57	0.66	10.61	4.82	1.00	0.31	0.42	1.09	1.67	0.62	0.30	2.92	0.14	0.04	0.03	74.6	0.26
A.II-3	0.47	1.00	2.78	0.17	1.82	11.53	0.84	0.46	2.11	0.42	0.26	0.49	1.37	0.54	0.23	0.14	5.43	0.35	0.02	0.09	78.4	0.09
OG.II-1	1.12	2.98	3.35	0.52	858	15.05	0.54	3.42	8.73	0.81	0.31	0.38	0.77	1.18	0.44	0.07	7.71	0.39	0.03	0.39	273.5	0.25
A.II-2	0.79	1.12	1.52	0.21	0.48	5.99	1.47	ND	7.51	1.39	0.04	0.05	0.13	0.04	ND	0.01	0.31	2.50	0.02	ND	8.29	ND
OG.II-2	1.32	0.38	2.10	0.21	32.7	0.89	0.14	17.70	0.21	0.23	0.09	0.12	0.47	0.29	0.09	0.02	2.27	0.20	0.02	0.03	74.3	0.14
A.I-I	1.20	1.63	1.16	0.11	452	1.30	0.23	0.16	1.99	0.11	0.09	0.17	0.26	0.18	0.15	0.01	0.50	ND	0.004	0.06	283.6	0.20
MB-1	3.77	1.07	2.77	0.43	1.29	5.54	1.02	33.94	0.51	0.63	0.02	0.29	0.74	0.63	0.13	0.05	4.85	1.74	0.06	0.07	13.89	0.23
MB-3	1.99	11.27	4.76	0.39	1.17	0.21	0.89	ND	0.04	0.04	0.005	0.003	0.03	0.13	0.02	0.006	0.095	ND	0.05	0.001	0.79	ND

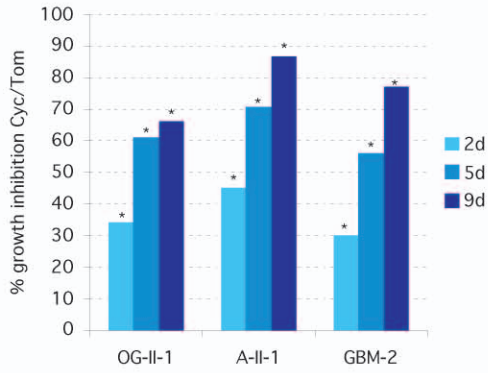
threshold up	0.4	0.7	1.50	0.15	24	10	1.2	4.30	1.1	0.50	0.15	0.35	1.00	1.2	0.4	0.3	13	0.5	0.15	0.07	50	0.2
threshold down	0.15	0.20	1.15	0.06	3	3.5	0.5	0.8	0.2	0.20	0.03	0.1	0.3	0.5	0.18	0.15	6	0.2	0.005	0.01	20	0.05
parietal ctx	0.21	0.28	1.31	0.11	5.77	4.99	0.93	1.28	0.46	0.38	0.08	0.28	0.77	0.88	0.34	0.20	10.03	0.37	0.02	0.04	25.77	0.14
frontal ctx	0.38	0.50	1.18	0.13	23.50	4.24	0.67	1.15	0.96	0.44	0.06	0.16	0.64	0.80	0.24	0.23	12.74	0.37	0.01	0.04	23.31	0.11
temporal ctx	0.28	0.48	1.33	0.11	3.44	8.52	1.04	4.02	0.58	0.31	0.10	0.28	0.86	0.66	0.33	0.24	12.11	0.32	0.10	0.03	38.52	0.08

Suppl. Fig. 2 Clement et al.

	Mesenchymal		Proneural		Proliferative		
	high YKL40	high CD44	high BCAN	low MELK	high CD133	low GFAP	high PCNA
GBM-1	0.35	0.06	0.10	0.02	0.87	8.86	0.23
GBM-2	0.30	0.08	0.10	0.02	5.98	234.98	0.20
GBM-3	0.04	0.07	0.15	0.05	3.67	206.12	0.32
GBM-4	0.01	0.05	0.35	0.09	1.47	179.01	0.38
GBM-5	0.34	0.20	0.18	0.03	4.70	220.04	0.53
GBM-6	0.41	0.18	0.25	0.07	11.42	553.54	0.74
GBM-7	0.43	0.18	0.20	0.08	43.55	254.80	0.35
GBM-8	0.19	0.08	0.13	0.04	0.16	53.95	0.22
GBM-9	0.01	0.02	0.03	0.01	4.37	17.95	0.40
GBM-10	0.14	0.06	0.06	0.02	8.11	117.17	0.11
GBM-11	0.22	0.04	0.04	0.02	5.02	39.35	0.10
GBM-12	ND	ND	ND	0.01	ND	ND	0.03
GBM-13	0.38	0.04	0.05	0.02	8.83	58.43	0.12
A.III-1	0.02	0.17	0.63	0.35	9.50	651.55	0.79
A.III-2	0.07	0.14	0.42	0.12	15.68	482.94	1.13
A.III-3	0.02	0.06	0.29	0.03	2.66	134.46	0.41
OG.III-1	0.28	0.25	0.10	0.10	ND	74.34	0.51
OG.III-2	0.06	0.12	0.50	0.07	20.22	444.45	0.74
OG.III-3	0.02	0.06	0.44	0.05	9.97	88.69	0.70
A.II-1	0.02	0.03	0.31	0.04	10.61	74.56	0.26
A.II-2	ND	ND	0.04	0.02	ND	8.29	ND
A.II-3	0.01	0.04	0.26	0.02	0.46	78.37	0.09
OG.II-1	0.01	0.06	0.31	0.03	3.42	273.53	0.25
OG.II-2	0.02	0.02	0.09	0.02	17.70	74.25	0.14
OG.II-3	0.04	0.17	0.86	0.04	12.45	561.59	1.00
AG.II-1	0.05	0.13	0.16	0.03	108.31	549.51	1.04
A.I-I	0.03	0.04	0.09	0.004	0.16	283.56	0.20
<i>threshold up</i>	0.03	0.17	0.15	0.15	4.30	50	0.2
<i>threshold down</i>	0.005	0.005	0.03	0.01	0.8	20	0.05

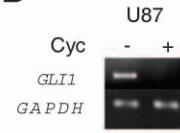
Supp Fig 3 Clement et al

A

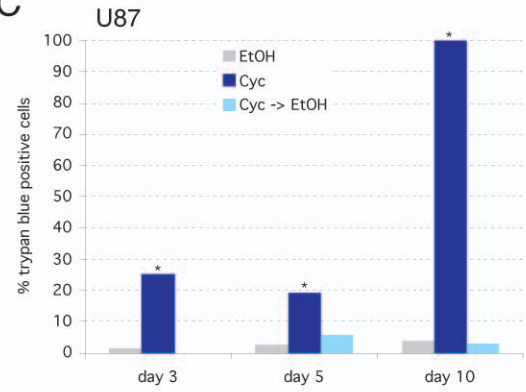


Suppl. Figure 4. Clement et al

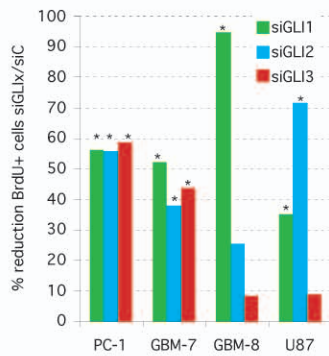
B



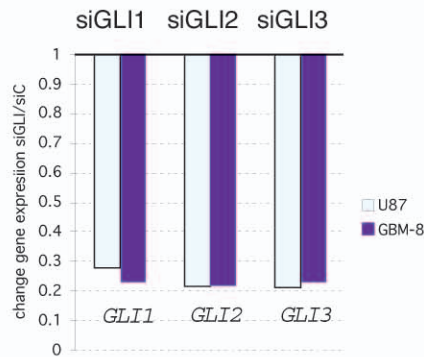
C



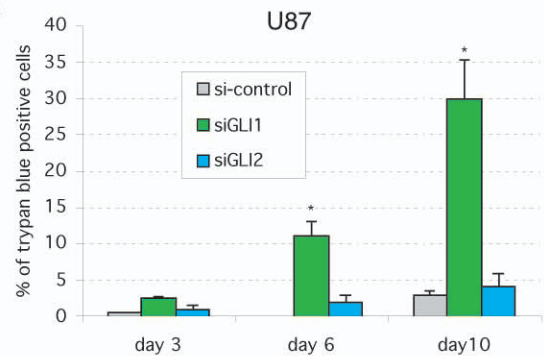
A



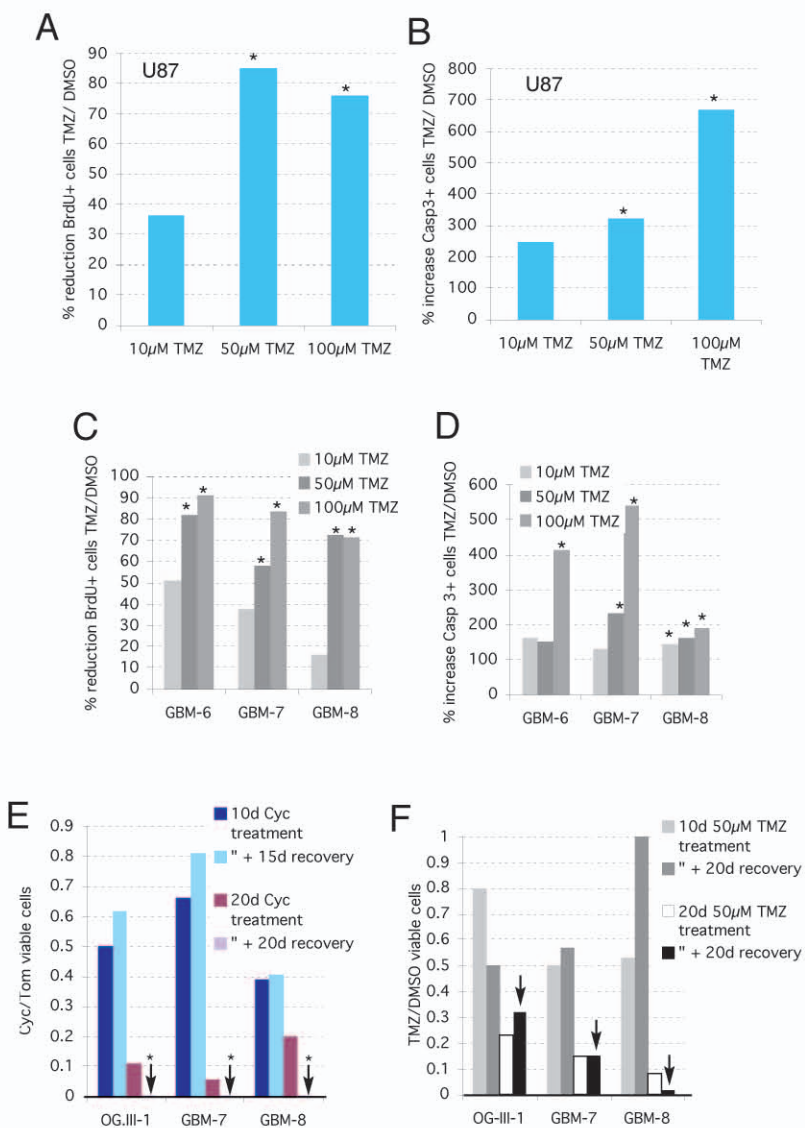
B



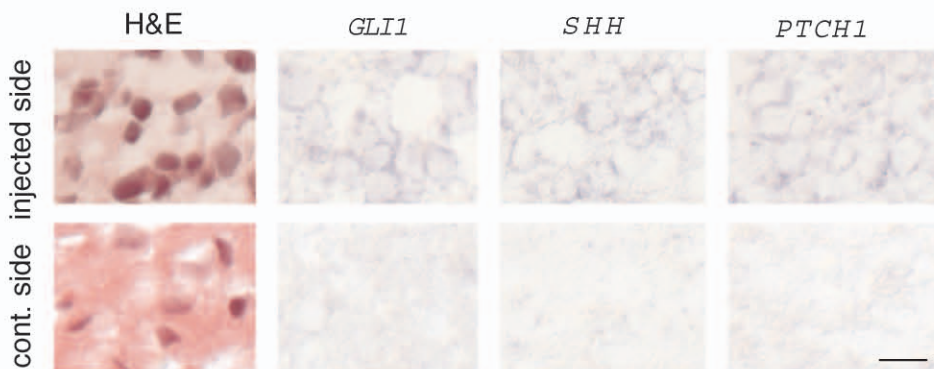
C



Suppl. Figure 5. Clement et al



Suppl. Figure 6. Clement et al



Suppl. Fig 7 Clement et al

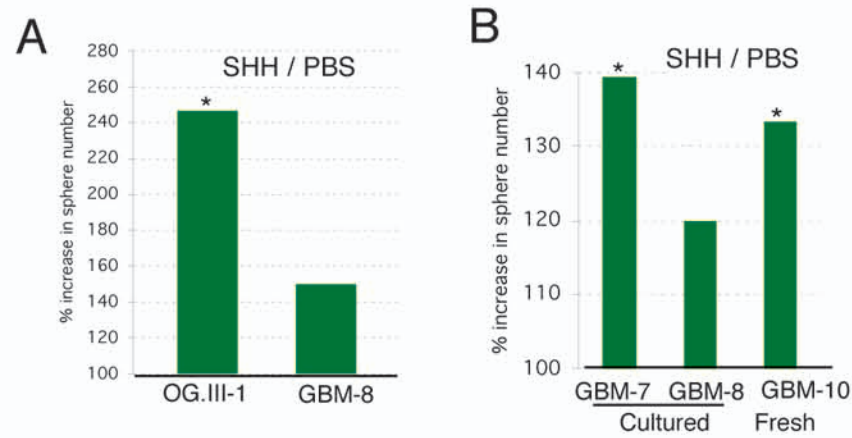
	NANOG	OCT.4	SOX2	BMI1	PCNA	GLI3	NCAM	GLI1	PTCH1	PDGFRA	NESTIN	GFAP	BCAN	PTEN	NOTCH1	OLIG2
GBM-14	0.32	0.23	0.19	0.03	0.21	1.78	0.20	1.17	0.32	0.18	2.32	0.13	0.03	0.09	0.46	0.08
GBM-10	0.43	0.27	0.28	0.02	0.19	1.64	0.34	0.77	0.35	0.22	2.18	0.24	0.17	0.03	0.75	0.29
GBM-8	0.23	0.29	0.31	0.03	0.23	3.47	0.34	7.74	1.18	0.57	5.02	0.19	0.21	0.27	3.43	1.64
GBM-7	0.30	0.32	0.34	0.03	0.28	2.00	0.35	0.83	0.40	0.36	2.28	0.37	0.21	0.08	1.90	0.32
GBM-6	0.37	0.15	0.33	0.05	0.27	2.02	0.17	0.53	0.47	0.11	3.82	0.05	0.11	0.01	0.39	0.22
A.III-2	0.24	0.52	0.45	0.03	0.35	1.28	0.34	0.93	0.30	0.45	0.68	0.20	0.11	0.03	0.67	0.29
OG.III-1	0.41	0.27	0.32	0.02	0.27	1.30	0.38	1.09	0.57	0.34	1.36	0.27	0.25	0.10	2.58	2.67

<i>mean</i>	0.32	0.29	0.32	0.03	0.25	1.93	0.3	0.8*	0.50	0.32	2.52	0.20	0.17*	0.05*	1.12*	0.28*
-------------	------	------	------	------	------	------	-----	------	------	------	------	------	-------	-------	-------	-------

	GLI2	DCX	NCS	YKL40	ABCG2	EGFR	SHH	CD133	NEUROD1
GBM-14	2.56	0.56	2.55	0.40	0.19	0.11	0.72	16.88	0.02
GBM-10	2.49	0.35	0.88	0.04	0.05	0.05	31.35	17.81	0.004
GBM-8	8.88	0.16	0.19	0.20	0.50	0.43	4.78	0.70	0.035
GBM-7	0.86	0.99	0.93	0.42	0.08	0.19	6.54	10.04	0.003
GBM-6	1.76	1.64	3.60	0.001	0.01	0.01	0.33	62.27	0.02
A.III-2	1.76	0.29	1.77	0.14	0.03	0.08	13.91	0.67	0.013
OG.III-1	ND	0.06	0.26	0.74	0.06	2.36	2.71	1.10	ND

<i>mean</i>	1.88*	0.58	1.45	0.32*	0.7*	0.14*	4.7*	14	0.025*
-------------	-------	------	------	-------	------	-------	------	----	--------

Suppl. Fig 8 Clement et al



Suppl. Figure 9. Clement et al

A

	GBM-6	GBM-7	GBM-8	GBM-10
GFAP	0.6	1.0	2.0	1.1
NCAM	1.1	0.9	2.0	0.8
NOTCH1	2.0	1.6	1.5	1.1
SHH	1.4	1.8	2.1	1.6
GLI1	0.7	1.1	1.4	1.4
GLI2	1.6	1.1	1.8	0.9
GLI3	0.8	1.2	1.4	1.0
PTCH1	0.9	0.8	1.1	0.7
NANOG	1.2	1.3	1.7	0.6
OCT.4	1.2	1.1	1.4	0.6
SOX2	0.7	0.8	1.9	0.6
NESTIN	1.8	1.1	3.5	0.4
BMI1	1.4	1.0	1.4	0.7
PDGFRA	0.3	1.0	1.6	0.02
OLIG2	0.8	0.6	2.9	0.7
BCAN	0.8	0.8	2.7	0.8
ABCG2	ND	0.7	2.4	1.8
NST	0.5	0.9	1.8	0.6
PTEN	0.5	1.1	1.2	0.7

B

	GBM-6	GBM-7	GBM-8	GBM-10
GFAP	Blue		Red	
NCAM			Red	
NOTCH1	Red	Red	Red	Red
SHH	Red	Red	Red	Red
GLI1			Red	Red
GLI2	Red		Red	Red
GLI3			Red	Red
PTCH1			Red	Red
NANOG			Red	Blue
OCT.4			Red	Blue
SOX2			Red	Blue
NESTIN	Red	Red	Red	Blue
BMI1	Red		Red	Blue
PDGFRA	Blue		Red	Blue
OLIG2		Blue	Red	Blue
BCAN			Red	Blue
ABCG2	Blue	Blue	Red	Blue
NST	Blue	Blue	Red	Blue
PTEN	Blue	Blue	Red	Blue
% 2ndary spheres	3	4	4	4
% CD133+ cells	19	7	6	2
% CD133+ spheres	6	10	14	10
Sphere quality	good	good	excellent	poor

Suppl. Fig. 10 Clement et al